Supplementary Material

Supplementary Methods

Colonies

In both locations, the 3xTgAD and the control colonies were maintained 'in-house' through the pairing of homozygous individuals. Mice were housed in cages of up to five, with same-sex and genotype cage-mates in a pathogen-free environment, kept at a 45-65% humidity, under a 12:12-hour light-dark cycle and room temperature, with *ad libitum* access to food and water.

Optogenetic surgery

Male 129sv/c57bl6 and 3xTgAD mice (~30 g, N = 19, N = 12 respectively) were anesthetized with a mixture of ketamine/xylazine (ketamine 75 mg/kg, xylazine 10 mg/kg). The head was shaved and cleaned with three wipes of Betadine® and ethanol (70%). Lidocaine was administered subcutaneously, *in situ* under the scalp. Each animal was kept on a warm pad to prevent hypothermia, and the head was positioned in a stereotaxic frame; protective ophthalmic gel was applied to avoid dryness. A portion of the scalp was removed to expose the skull. The distance between Bregma and Lambda was measured and compared to the standard 4.2 mm reported in the mouse brain atlas. Any deviation from 4.2 mm allowed a proportional adjustment for craniotomy coordinates. Small craniotomies were performed above the left hemisphere with a drill (burr tip 0.9 mm^2) at -2.8 from bregma, +4.2 from the midline. Virus injection into ENTl was carried out through this craniotomy at -2.8 to -2.7 mm from the brain surface and cannula positioning reached -2.6 mm from the surface. Coordinates were taken according to the Paxinos mouse brain atlas [1]. An injection of adeno-associated virus (AAV) was performed in the target location using a precision pump (KD Scientific Inc., Harvard Bioscience) with a 10 µl NanoFil syringe with a 33-gauge beveled

needle (NF33BV-2). The AAV used [2], AAV5-CaMKIIa-hChR2(H134R)-mCherry ($N_{controls}$ = 10, N_{3xTgAD} = 12) or AAV5-CaMKIIa-mCherry ($N_{mCherry\text{-}controls}$ = 9), titer 1-8x10^{12} vg/ml, were acquired from Vector Core at the University of North Carolina (USA). A total volume of 0.75 µl of the vector was injected in each mouse at a rate of 0.15 µl/min. The injector was kept in location for 10 minutes after injection completion to preclude backflow. After the extraction of the needle, a fiber optic cannula (diameter 200 µm, 0.39 NA, length according to the injection site, diameter 1.25 mm ceramic ferrule) was lowered to the targeted region (Laser 21 Pte Ltd, Singapore; Hangzhou Newdoon Technology Co. Ltd, China). The cannula was fixed in place with dental cement (Meliodent rapid repair, Kulzer). Buprenorphine was administered post-surgically to each animal. Animal recovery took place on a warm pad.

Anatomical gene expression atlas comparison

The spatial expression profile for 4117 genes was obtained from the anatomical gene expression atlas database using the application programming interface from the AIBS [3]. The spatial correlation between the ReHo second-level statistical map and each of the genes was estimated using Pearson's correlation (*fslcc*). ReHo-gene correlations were ranked and tested for enrichment of biological processes using Gene Ontology enRIchment anaLysis and visuaLizAtion tool (GOrilla, http://cbl-gorilla.cs.technion.ac.il/) [4,5]. Enrichment was tested with Fisher's Exact test with FDR correction.

Electrophysiological recordings *in vivo*: anesthesia and surgical procedure

Anesthesia was induced via intraperitoneal injection of urethane (1.5-1.7 g/kg of 30% w/v solution prepared in 0.9% saline, ethyl carbamate, Sigma, UK). An additional dose of urethane (50 µl of 10% w/v urethane solution prepared in 0.9% saline) was administered if complete areflexia was not reached after 40 minutes from the first injection. Mice were mounted and

fixed in a stereotaxic frame and mouse adapter (Kopf 1430, USA) to immobilize the head prior to surgery. Body temperature was maintained around 37°C throughout the duration of the experiment with the use of a homoeothermic blanket (Harvard, UK) and a thermistor probe placed underneath the abdomen. A midline scalp incision was made, and the skin retracted to expose the skull. After identifying Bregma and Lambda, the distance between these two landmarks was measured and compared to the standard 4.2 mm reported in the mouse brain atlas [1]. Any deviation from 4.2 mm allowed a proportional adjustment for craniotomy coordinates to improve the accuracy of electrode placement. Craniotomies were made above the left hemisphere using a 0.9 mm drill bit (Fine Science Tools, Germany) and a high-speed handheld drill (Foredom, USA). Care was taken to maintain the craniotomy sites moist during the whole surgical procedure with sterile saline. Coordinates for craniotomy and electrode placement were marked onto the skull, relative to Bregma and the midline for recording in BLA (Bregma: AP -2.5 mm, ML: +2 mm) and DG (Bregma: AP -3.5 mm, ML: +2.5 mm), as well as stimulation of ENTl (Bregma: AP -2.8 mm, ML: +4.2 mm). Recording electrodes consisted of 32-contact probes, each laid out as 2 shanks of 16 electrodes that were 500 μm apart with 100 μm between recording points (A2x16-10-500-100-413, NeuroNexus Technologies, MI). The probe shanks were coated in Vibrant CM-DiI (Sigma, UK) cell-labeling solution to allow post-mortem localization of their location with fluorescence microscopy.

Probes were then lowered to target locations (BLA target was 4 mm ventral from the brain surface at a 15° angle from vertical in the coronal plane; the DG target was also 4 mm ventral to brain surface but along a vertical plane) to record brain activity and evoked responses during different stimulation protocols. The stimulation electrode consisted of paired twisted, diameter 125 μm Teflon-insulated stainless-steel wires (Advent RM, UK) and was inserted an initial 3 mm from the brain surface in one step and then slowly lowered further during continuous

application of stimulating pulses (50 ms PPS, 300 μA, 0.2 ms duration pulses) until the expected responses in DG and BLA were seen on an oscilloscope.

Electrophysiological recordings *in vivo*: data acquisition

Data were recorded on a Recorder64 system (Plexon Inc, USA), and saved for offline analysis. Electrodes were connected to a head stage amplifier (fixed gain of x20) and then to a preamplifier for a total gain of x500. Field excitatory postsynaptic potentials (fEPSPs) were recorded at a sampling rate of 5 or 10 kHz using a 12-bit A/D converter and then stored for offline analysis. A low pass filter (1 kHz) was applied to attenuate spiking activity. Electrical stimuli were delivered by a constant-current stimulator (DS3, Digitimer, UK), triggered by analog 5 V square wave pulses from a National Instruments PCI card (PCI-6071E). Timings and types of stimuli to be delivered were controlled through custom-written programs in LabVIEW (v8, National Instruments, USA). Stimulus duration was fixed at 200 μs throughout. Two different protocols of stimulation were performed: Input/Output, for the Input/Output curve (IOC) analysis and PPS for the PPI analysis. In each mouse, the channel with the most distinctive response (as revealed through current source density analysis *post hoc*; see below) was selected for further analysis.

Electrophysiological recordings *in vivo*: stimulation protocols - Input/output curve

The IOC reflects the functional strength of synaptic connectivity: by applying different current intensities, it is possible to analyze how the response (Output voltage) changes as a function of input strength (Input current). The range of current intensities used here was 180, 300, 450 and 600 μA.

Electrophysiological recordings *in vivo*: stimulation protocols - Paired-pulse stimulation

To measure short-term synaptic plasticity, stimulus current was set to half-maximum of the response obtained in the BLA IOC paradigm, i.e., ~300 μA, and paired-pulses were delivered at this current with different paired-pulse intervals for 20 repetitions each. The range of intervals was 20, 50, 100, 200, 500 and 1000 ms.

Electrophysiological recordings *in vivo*: data analysis

For the IOC protocol, stimulation at each current intensity was repeated 20 times (runs), the initial slope of the fEPSP response measured for each repetition and then these 20 values were averaged. The mean response to each current step for each mouse was used to plot the IOC of response to current intensity by genotype, age, and ROI. For the PPS protocol, the slope of the initial fEPSP response on a selected channel was measured from responses to both stimuli in each pair. For each pair, the fEPSP slope to the second stimulus (P2) was normalized to that of the first (P1) and expressed as PPI ratio (see equation 1, below), such that positive values indicate synaptic paired-pulse facilitation (PPF) and negative values synaptic PP depression (PPD).

$$PPI = (P2 - P1) / P1 \quad (1)$$

Whole-cell patch recording of acute brain slices

Mouse brains were rapidly removed after decapitation and placed in high sucrose ice-cold oxygenated artificial cerebrospinal fluid (ACSF) containing the following (in mM): 230 sucrose, 2.5 KCl, 10 $MgSO_4$, 0.5 $CaCl_2$, 26 $NaHCO_3$, 11 glucose, 1 kynurenic acid, pH 7.3, 95% O_2 and 5% CO_2. Coronal brain slices were cut at a thickness of 250 μm using a vibratome (VT1200S; Leica Biosystems) and immediately transferred to an incubation chamber filled with ACSF containing the following (in mM): 119 NaCl, 2.5 KCl, 1.3 $MgCl_2$, 2.5 $CaCl_2$, 1.2 NaH_2PO_4, 26 $NaHCO_3$, and 11 glucose, pH 7.3, equilibrated with 95% O_2 and 5% CO_2. Slices

were allowed to recover at 32°C for 30 minutes and then maintained at room temperature. Experiments were performed at room temperature. Whole-cell patch-clamp recordings were performed on ENTl pyramidal cells expressing ChR2-mCherry and were visualized using a CCD camera and monitor. Pipettes used for recording were pulled from thin-walled borosilicate glass capillary tubes (length 75 mm, outer diameter 1.5 mm, inner diameter 1.1 mm, WPI) using a DMZ Ziets-Puller (Zeitz). Patch pipettes (2–4 MΩ) were filled with internal solution containing (in mM): 105 K-gluconate, 30 KCl, 4 $MgCl_2$, 10 HEPES, 0.3 EGTA, 4 Na-ATP, 0.3 Na-GTP, and 10 Na_2-phosphocreatine (pH 7.3 with KOH; 295 mOsm), for both voltage- and current-clamp recordings.

Photostimulation (460 nm) was delivered by an LED illumination system (pE-4000). Several trains of a square pulse of 20 ms duration with 5, 10, and 20 Hz, were delivered respectively under current-clamp mode (I = 0) to examine whether the neurons were able to follow high-frequency photostimulation. After different frequencies of photostimulation were completed, neurons were shifted to voltage-clamp mode (at -60 mV), and a prolonged square pulse of 500 ms duration was delivered, to further confirm whether ChR2-induced current could be seen in the recorded neurons. The access resistance, membrane resistance, and membrane capacitance were consistently monitored during the experiment to ensure the stability and the health of the cell.

Immunohistochemistry for AT8 and 6e10

Immunohistochemical analyses were performed as described previously in [6]. Brains of $N_{controls}$ = 6 (2 per age point: 3, 6 and 10 months of age) and N_{3xTgAD} = 6 (2 per age point: 3, 6 and 10 months of age) were fixed by perfusion with 4% paraformaldehyde (PFA) in 0.01 M phosphate buffer saline (PBS) and then in PFA and 30% sucrose for 48 h at 4°C. Fixed brains were cut on a microtome (CM3050S, Leica Microsystems, Nussloch, Germany) into 45 μm-thick

sections and collected into a cold cryoprotectant solution (80 mM K_2HPO_4, 20 mM KH_2PO_4, 154 mM NaCl, 0.3 g/ml sucrose, 0.01 g/ml polyvinylpyrrolidone, 30% vol/vol ethylene glycol). Sections were washed 5 times for 3 minutes in 1 x PBS and blocked in 5% FBS with 0.1% Triton X-100 for 1 hour, followed by overnight incubation with the primary antibody in blocking solution at 4°C. These brain sections were then immunostained with primary antibodies against Aβ (6e10, Covance Research Products Inc Cat #SIG-39300-1000 RRID: AB_10175637) and phospho-tau (AT8 ThermoFisher Scientific, Cat. #MN1020). After the primary antibody binding step sections were washed 5 times in 1 x PBS for 3 min and then incubated with anti-mouse Alexa 488 or anti-rabbit Alexa 594 for 2 hours followed by washing 3 times with 1 x PBS for 3 minutes. Sections were then mounted with DAPI plus mounting media on slides. All pictures were taken by using a confocal microscope with a 40× objective and a zoomed-in version is displayed next to each section (Figure 2a-l, right panels).

***Ex vivo* histology**

After the completion of the experiments, animals were injected with an overdose of ketamine/xylazine and transcardially perfused with PBS (0.01 M) followed by 4% PFA in 0.01 M PBS. After extraction, the brain was post-fixed in 4% PFA overnight. Brain sections of 50 µm were made with a vibratome (VBT1200s, Leica) and fluorophore expression, together with Hoechst staining, was checked through a confocal microscope Ti-E; DS-Qi2; Fluorescence, SBIC-Nikon Imaging Center, Singapore) for anatomical confirmation of viral injection and fiber optic cannula positioning (Figure 4).

Statistics and data availability

Electrophysiology in vivo: For both the IOC and PPS results, statistical analysis was performed using the statistical software R 3.6.1 (The R Foundation for Statistical

Computing). Responses to the IOC (initial slope for P1) and PPI (ratio between P2 and P1) paradigms in BLA and DG at the two age points were analyzed separately with a linear mixed model analysis, using ROI, age, genotype, amplitude/intervals (amplitude for IOC and interval for PPS), and their mutual interactions as fixed effects and animal intercepts and run repeats as random effects using R package lme4. Interaction effects were determined using a likelihood ratio test. A *post hoc* analysis was performed after a general linear hypothesis test using contrast to determine genotype effects at each stimulation amplitude or interval. Correction for multiple comparisons was implemented during the contrast analysis using the R package multcomp [7,8]. Data were plotted as mean ± 1 standard deviation (SD).

Supplementary Figures

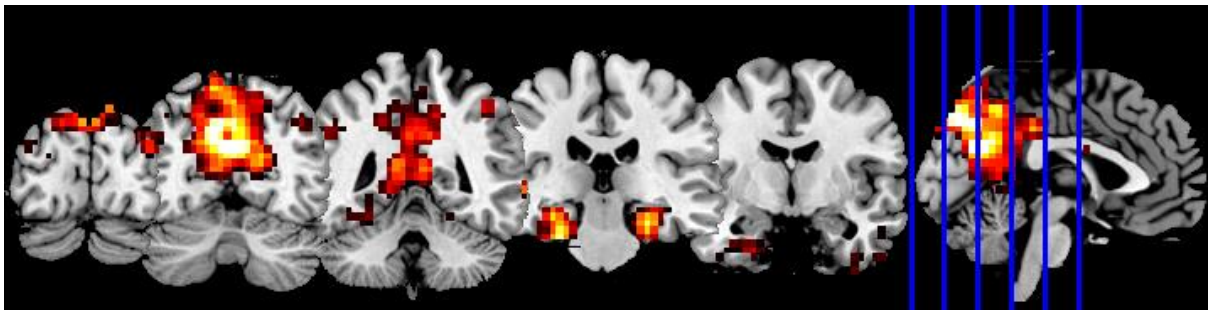

Figure S1 | Spatial maps of common regions involved in Alzheimer's as revealed by literature meta-analysis.
The regions affected by AD, revealed by the query, encompass the parietal, precuneus and temporal lobe regions.

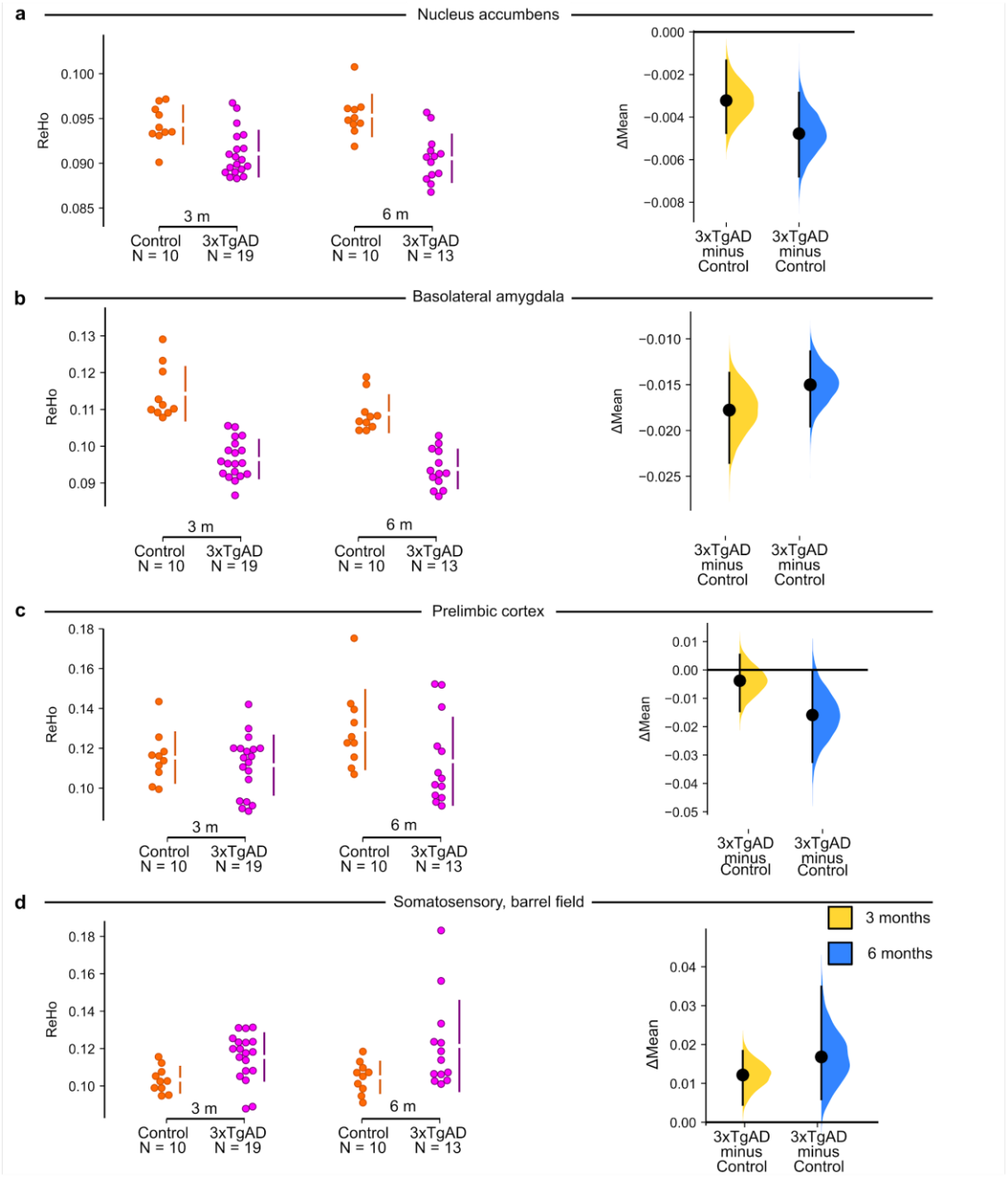

Figure S2 | ReHo values extracted in selected ROIs show functional connectivity changes in 3xTgAD. 3xTgAD mice show deficits in ReHo in regions encompassing **a)** the ACB ($\Delta mean_{3months}$ = -0.110 [-0.154, 0.068], $\Delta mean_{6months}$ = -0.152 [-0.199, -0.107]); **b)** the BLA ($\Delta mean_{3months}$ = -0.066 [-0.110, -0.025], $\Delta mean_{6months}$ = -0.061 [-0.115,-0.011]); **c)** the mPFC, prelimbic reported as example ($\Delta mean_{3months}$ = -0.004 [-0.015, -0.005], $\Delta mean_{6months}$ = -0.016 [-0.032, 1.93E-05]); **d)** increase in ReHo was found in somatosensory areas (SSp-bfd, $\Delta mean_{3months}$ = 0.0833 [0.0192, 0.149], $\Delta mean_{6months}$ = 0.112 [0.0587,0.157]) suggests that functional connectivity deficits in 3xTgAD might be network-specific to AD-vulnerable regions. ACB: nucleus accumbens; BLA: basolateral amygdala; ReHo: regional homogeneity

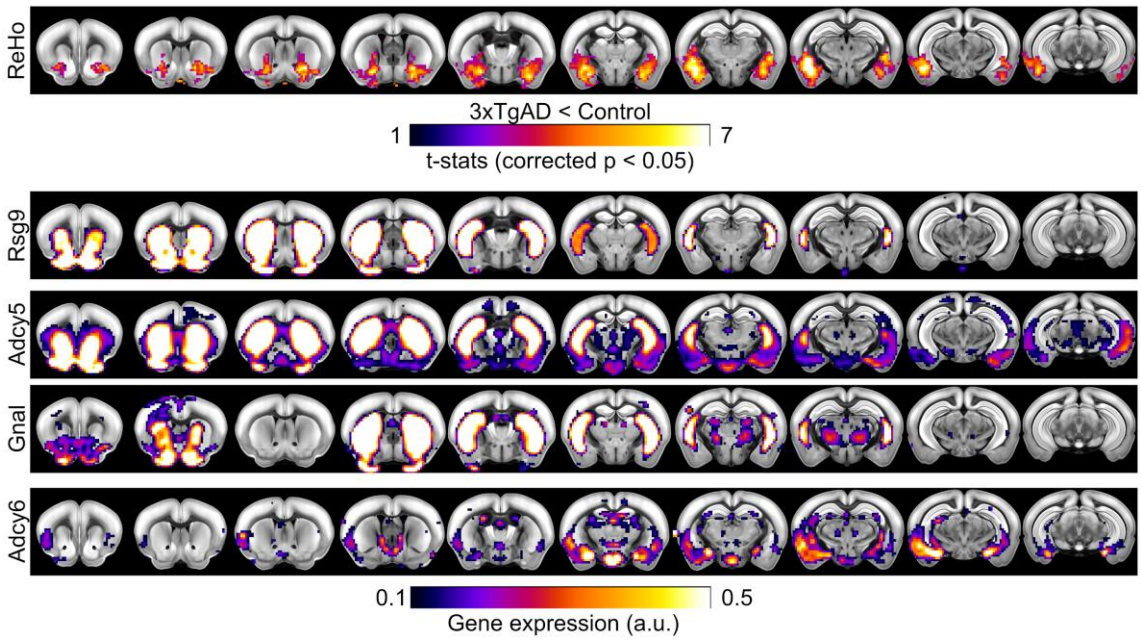

Figure S3 | Correlated gene expression.
Selected gene expression maps derived from the Anatomic Gene Expression Atlas present mild correlations (r range [0.2 - 0.14]) with ReHo deficits in 3 months old 3xTgAD.

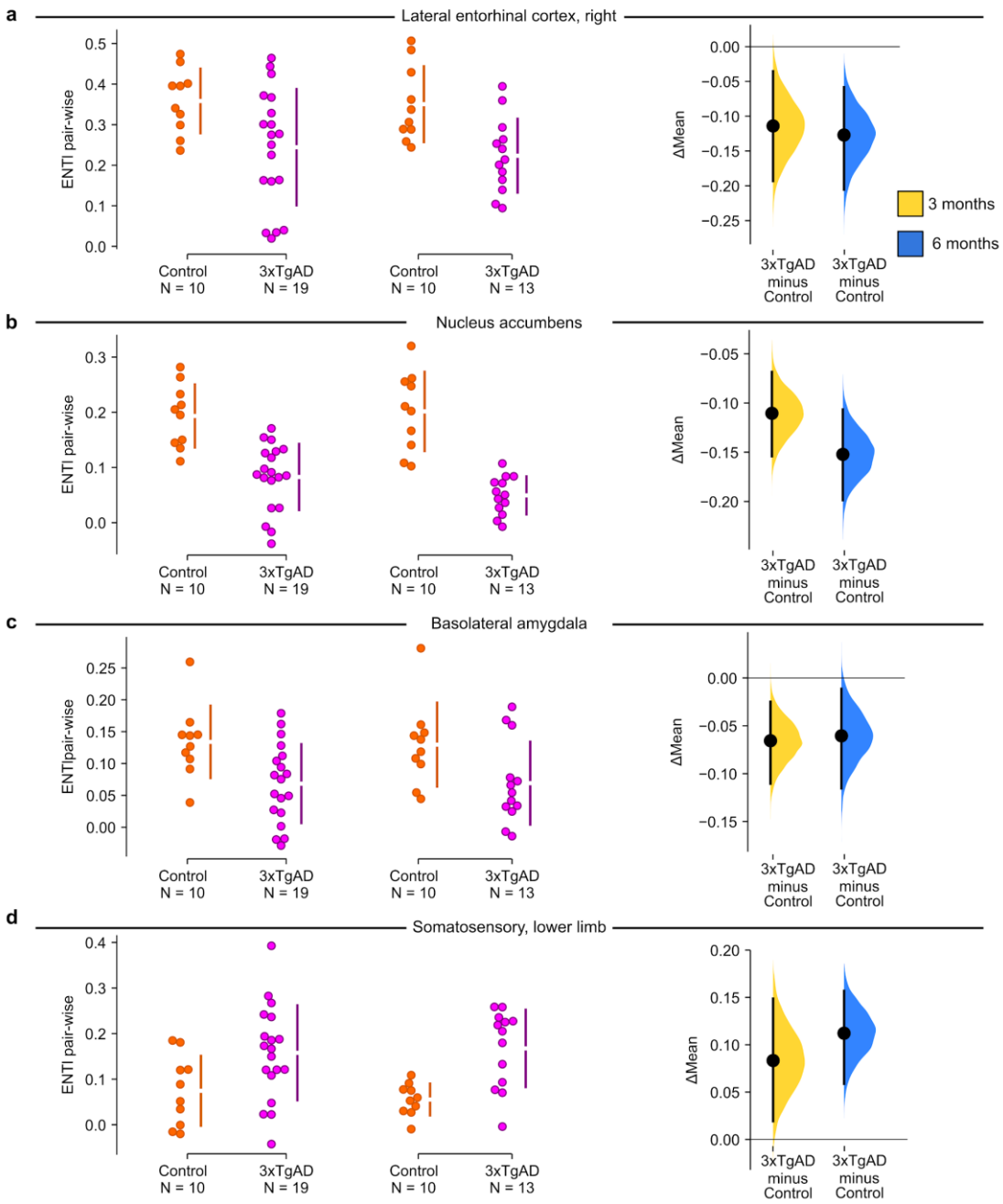

Figure S4 | Pair-wise ROI interactions relative to the left-hemisphere ENTl.
Compared to the left ENTl, 3xTgAD mice show a decrease in functional connectivity in the right ENTl **(a)**, ACB **(b)** and BLA **(c)**. These results show consistent trends as in whole-brain ReHo, highlighting the relevance of ENTl as a central hub for functional connectivity changes in 3xTgAD. **d)** Functional connectivity in somatosensory regions is increased in 3xTgAD compared to controls, in pair-wise interaction with left ENTl.

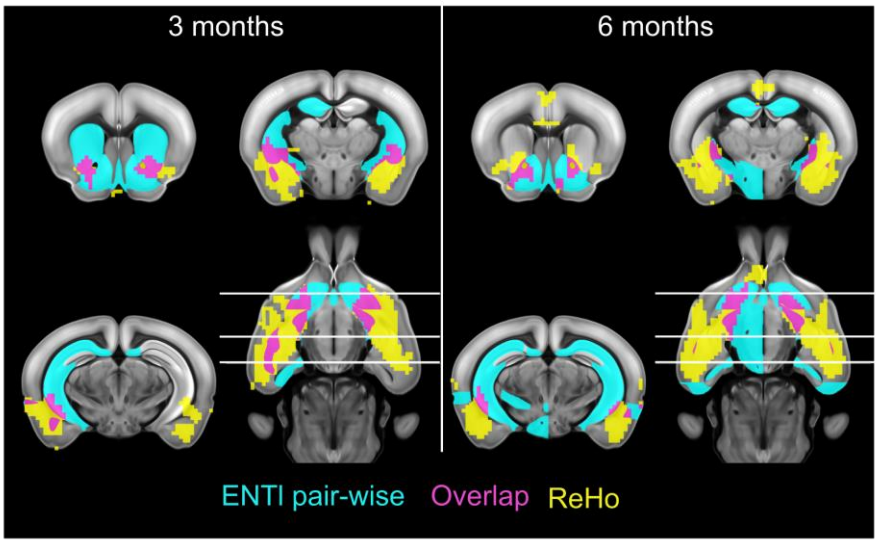

Figure S5 | Restricted pair-wise ENTl at 3 and 6 months overlapped with ReHo.
The overlap (pink) between ReHo (yellow) and pair-wise interactions between ENTl and whole-brain regions (cyan) resulted in major hotspots of interest, consistent across ages.

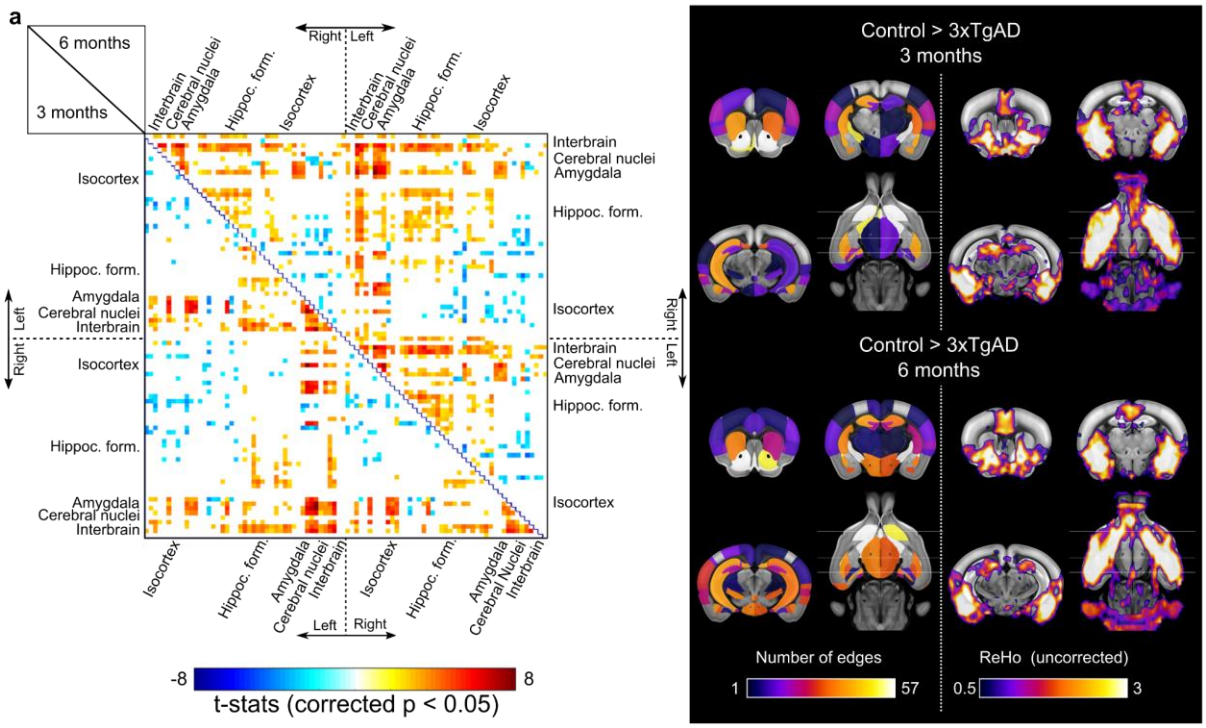

Figure S6 | Whole-brain NA at 3 months and 6 months and overlap with ReHo analysis.
a) Half-matrices of whole-brain network analysis show deficits in 3xTgAD at 3 and 6 months of age. **b)** Overlap of ReHo results (uncorrected) with NA spatial maps highlight common regions showing deficits in functional connectivity, such as the amygdaloid/cerebral nuclei (e.g. BLA and ACB) and hippocampal formation (e.g. ENTl). ReHo: regional homogeneity; NA: network analysis; ENTl: lateral entorhinal cortex; BLA: basolateral amygdala; ACB: nucleus accumbens.

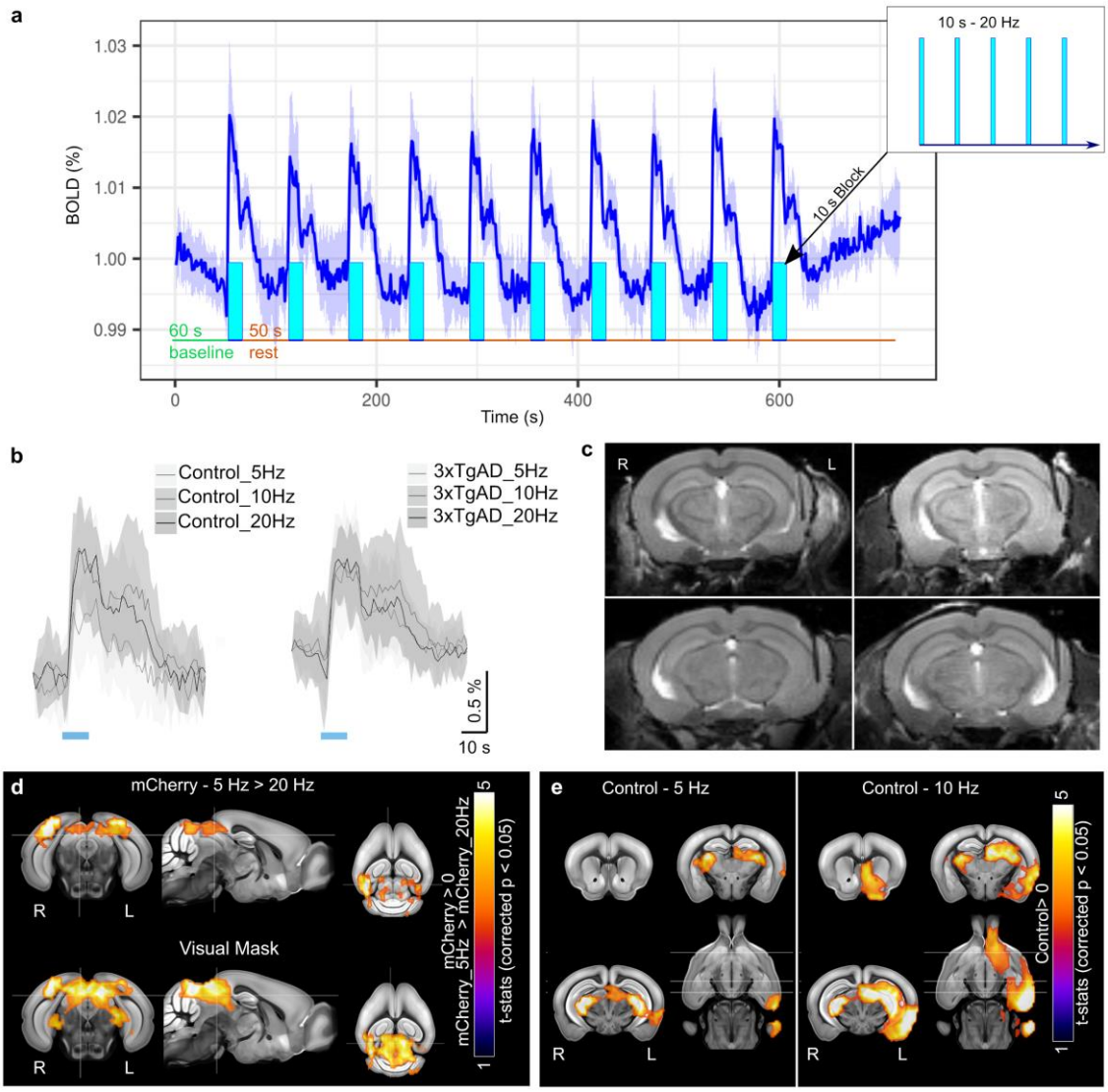

Figure S7 | Experimental design for optogenetic stimulation and control validation.
a) Stimulation design consisted of 50 s baseline and subsequent 10 blocks of 5, 10, or 20 Hz-pulses for 10 s, alternated by 50 s of rest with no stimulation; stimulation protocols were provided in random order. **b)** Average BOLD response for the 10 blocks of stimulation across frequencies for controls and 3xTgAD (left and right respectively), represented as mean ± SD. **c)** The anatomical scan shows the fiber positioning in 4 mice from the experimental group. **d)** Top: Two-sample t-test in mice transfected with mCherry shows that only lower frequencies, i.e. 5 Hz, engage a stronger response in the visual system, compared to 20 Hz stimulation. Bottom: Response derived from a 5 Hz stimulation protocol was used to mask the regions that responded positively to visual stimulation. **e)** Mice injected with ChR2 show response to low frequencies, i.e. 5 and 10 Hz, here shown as the control group at 3 months of age. The response to 20 Hz stimulation was chosen for the rest of the analyses.

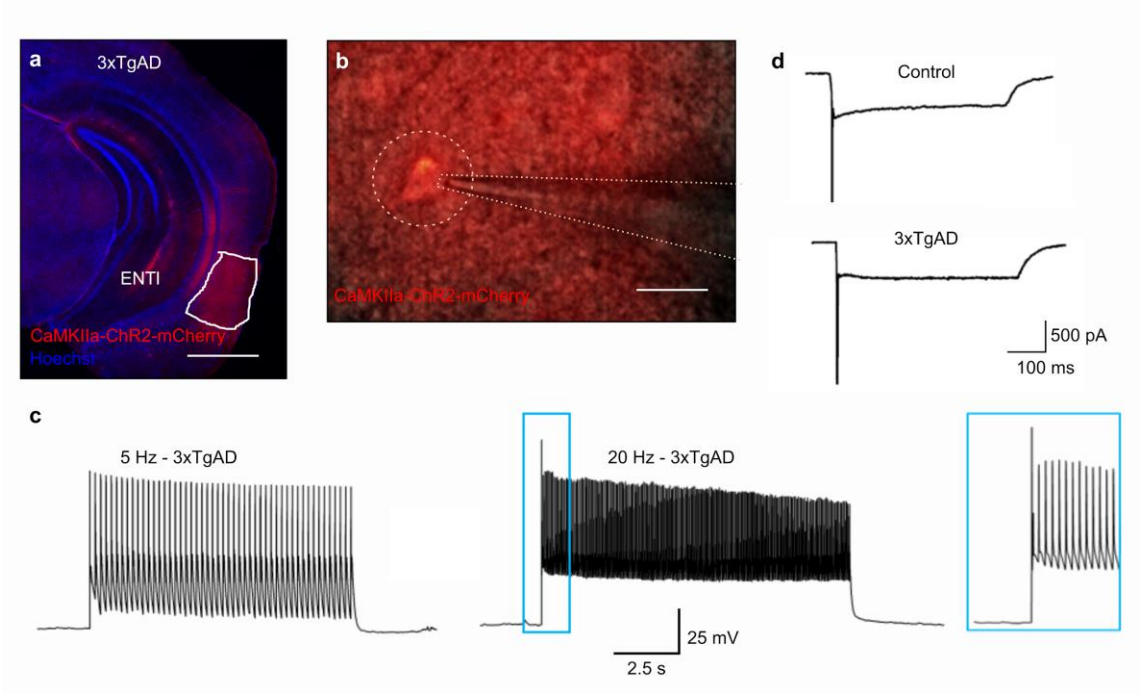

Figure S8 | Optogenetic validation of pyramidal neurons in ENTl.
a) Histological evidence for opsin expression in 3xTgAD mice co-stained with Hoechst neuronal cell bodies. Scale bar: 1000 µm.**b)** whole-cell patch-clamping in a ChR2-expressing pyramidal neuron in the ENTl. Scale bar: 25 µm. **c)** 5 and 20 Hz stimulation of the patched neuron shows faithful frequency-gated activity. **d)** Prolonged photostimulation (500 ms) applied under voltage-clamp mode (-60 mV) shows an initial action potential spike and a ChR2-induced inward current.

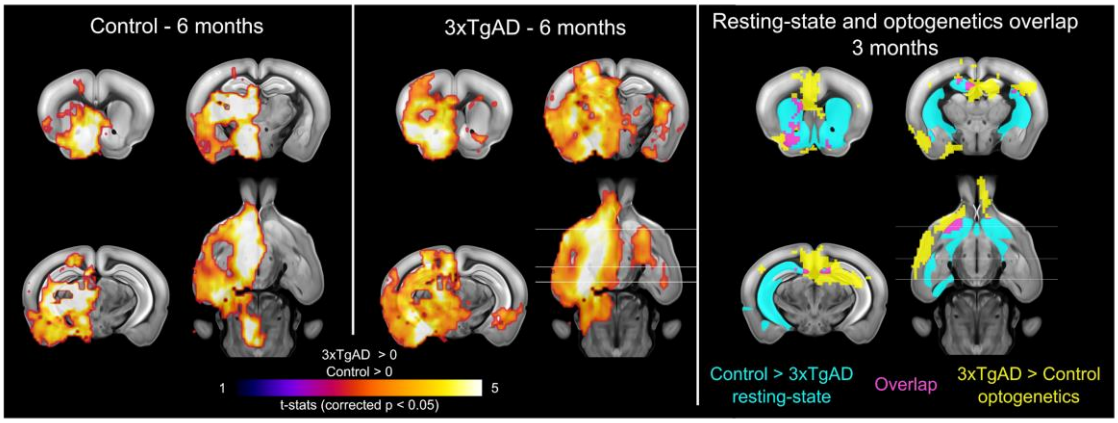

Figure S9 | Optogenetically-locked BOLD response in control and 3xTgAD mice at 6 months and the overlap with resting-state functional connectivity at 3 months.
Left and middle panels indicate the one-sample t-test for stimulation-locked BOLD response in the control and 3xTgAD cohorts, respectively ($p < 0.05$ corrected), highlighting activation in key regions related to ENTl projections, i.e., HIP, BLA, ACB. The right panel indicates resting-state functional connectivity analysis (cyan) and optogenetically-evoked response (yellow) highlights overlapping *loci* for the decrease in functional connectivity at rest and potentiated response during stimulation (pink) at the 3-month-old age point.

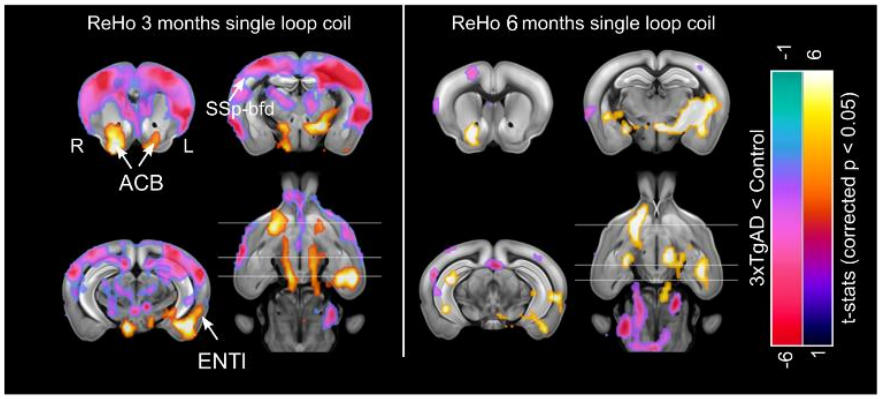

Figure S10 | Resting-state fMRI with single-loop coil reveals similar patterns of functional connectivity deficits in 3xTgAD.
ReHo analysis of rsfMRI with the single-loop coil, acquired before the ofMRI protocols, reveals similar loss of coherence in AD-vulnerable brain regions, e.g., ENTl, ACB. The increase in ReHo in somatosensory areas is also in line with the results reported with the cryogenic coil. 3 months: $N_{controls} = 10$; $N_{3xTgAD} = 12$; 6 months: $N_{controls} = 8$; $N_{3xTgAD} = 10$. ENTl: lateral entorhinal cortex; ACB: nucleus accumbens; SSp-bfd: somatosensory barrel field cortex; ReHo: regional homogeneity.

Table S1: Animal breakdown for the experimental procedures.

	3 months		**6 months**		**10 months**
	Control	3xTgAD	Control	3xTgAD	3xTgAD
RsfMRI	10▸	19▸▸	10▸	13▸▸	-
OfMRI-ChR2	10•	12••	8•	10••	-
OfMRI-mCherry	9	-	-	-	-
PPS	7	6	4	4	-
IOC	5	4	4	3	-
Slice electrophysiology			4•	5••	-
Slice optogenetics	1	1	-	-	-
Viral expression histology	1 (ChR2-mCherry)• 1 (mCherry)	1••	-	-	-
Immunohistochemistry	2	2	2	2	2
ELISA	2•	1••	2•	4••	1

RsfMRI and ofMRI experiments were conducted on different cohorts of animals. Within each cohort, longitudinal experiments between 3- and 6-months age points were performed. Subgroups of the experimental animals that previously underwent fMRI experiments, were then used for slice electrophysiology, viral expression validation, and ELISA tests. The same symbol represents animals belonging to the same cohort or a subgroup of the same cohort. Electrophysiological experiments *in vivo* were conducted on different cohorts, being this a non-recovery procedure. Immunohistochemistry stainings were performed on a separate sample of mice.

Table S2: Intrinsic properties of granule cells in the dentate gyrus and pyramidal cells in the infralimbic cortex, part of the medial prefrontal cortex.

	Dentate gyrus			Infralimbic cortex		
	Controls N = 4, n = 29	3xTgAD N = 5, n = 18	p-value (M-W)	Controls N = 4, n = 10	3xTgAD N = 5, n = 11	p-value (M-W)
Rm (mV)	-74.54±0.7242	-76.66±1.029	ns	-52.42±2.827	-54.71±3.149	ns
Rheobase (pA)	79.83±6.231	69.44±6.591	ns	37±8.95	24.55±3.659	ns
Threshold (mV)	-33.38±1.554	-36.38±1.919	ns	-35.69±0.5727	-34.58±1.228	ns
AP latency (ms)	238±40.01	343.3±56.88	ns	94.81±28.06	174.2±33.35	ns
AP amplitude (mV)	97.06±2.129	91.59±2.219	ns	72.99±2.284	70.34±2.871	ns
AHP (mV)	-11.35±0.8297	-10.17±1.241	ns	-10.9±1.653	-10.73±0.9142	ns
AHP latency (ms)	5.015±0.2014	4.794±0.3514	ns	16.88±3.091	55.6±13.21	0.0028 (**)
Half-width (ms)	1.321±0.0424	1.242±0.0472	ns	2.27±0.1154	2.862±0.2157	0.0079 (**)

Rheobase, threshold, action potential (AP) latency, AP amplitude, afterhyperpolarization (AHP), AHP latency, and AP half-width were measured from the first trace showing action potentials (Rheobase trace). N = number of animals, n = number of cells. The values represent mean value with SEM and the statistical significance by asterisks (* $p < 0.05$, ** $p < 0.01$ by Mann-Whitney U test).

Table S3: Number of action potential evoked by various current injections.

	Dentate gyrus			Infralimbic cortex		
Current injection (pA)	Controls N = 4, n = 29	3xTgAD N = 5, n=18	p-value (M-W)	Controls N = 4, n = 10	3xTgAD N = 5, n = 11	p-value (M-W)
20	na	na	na	1.8±0.7572	2.182±0.6851	ns
40	0.1034±0.076	1.556±0.879	ns	4±1.229	6±0.9723	ns
60	0.5517±0.236	3.556±1.322	0.029 (*)	6.2±1.724	9.636±0.8008	ns
80	2.621±0.5985	6.056±1.652	ns	7.8±1.825	11.45±0.9757	ns
100	4.345±0.7773	8.5±1.801	ns	9.2±1.611	12.55±1.012	ns
120	5.241±1.013	10.39±1.91	0.0214 (*)	8±1.366	13.82±1.094	0.0036 (**)
140	6.138±1.24	10.83±1.526	0.0078 (**)	8.4±1.392	13.45±1.268	0.0204 (*)

The number of action potentials was counted in granule cells in the dentate gyrus and pyramidal cells in the infralimbic cortex from the various current injections (20 – 140 pA). N = number of animals, n = number of cells. The values represent mean value with SEM and the statistical significance was presented with asterisks (* $p < 0.05$, ** $p < 0.01$ by Mann-Whitney U test).

Supplementary References

1. Paxinos G, Franklin KBJ. *The Mouse Brain in Stereotaxic Coordinates*. Gulf Professional Publishing, 2004.

2. Deisseroth K. Optogenetics. *Nat. Methods.* 2011; **8**: 26–29.

3. Ng L, Bernard A, Lau C *et al.* An anatomic gene expression atlas of the adult mouse brain. *Nat. Neurosci.* 2009; **12**: 356–362.

4. Eden E, Navon R, Steinfeld I *et al*. GOrilla: a tool for discovery and visualization of enriched GO terms in ranked gene lists. *BMC bioinformatics* 2009; **10**: 48.

5. Eden E, Lipson D, Yogev S *et al*. Discovering motifs in ranked lists of DNA sequences. *PLoS Comput. Biol.* 2007; **3**: e39.
6. Baek SH, Park SJ, Jeong JI *et al.* Inhibition of Drp1 Ameliorates Synaptic Depression, Aβ Deposition, and Cognitive Impairment in an Alzheimer's Disease Model. *J. Neurosci.* 2017; **37**: 5099–5110.

7. Bates D, Mächler M, Bolker B *et al*. Fitting Linear Mixed-Effects Models Using lme4. *J. Stat. Softw.* 2015; **67**. doi:10.18637/jss.v067.i01

8. Bretz F, Hothorn T, Westfall P. *Multiple Comparisons Using R*. CRC Press, 2016.